Performance Analysis and Protocol Design for Multipacket Reception in Wireless Networks

ZHENG, Pengxuan

A Thesis Submitted in Partial Fulfillment

of the Requirements for the Degree of

Master of Philosophy

in

Information Engineering

January 2007


香港中文大學
大學
圖書館系統
03 JAN 2008
UNIVERSITY
LIBRARY SYSTEM
THE CHINESE UNIVERSITY OF HONG KONG

Abstract

A collision resolution scheme is vital to the performance of a random-access wireless network. Many schemes employ exponential backoff (EB) to adjust the transmission attempt rate according to the changing traffic intensity. Previous work on exponential backoff was mostly based on the conventional single-packet-reception model where only one packet can be successfully received at any one time. With mutipacket reception (MPR) enhancement at the physical layer, however, the medium-access-control (MAC) layer will behave differently from what is commonly believed. In this thesis, we analyze the performance of EB based on an MPR model, in which multiple packets can be received successfully at one time. The model in this thesis covers both finite and infinite population sizes. It is general enough to encompass most existing practical systems, specifically systems with carrier-sensing and those without. Our analysis reveals the effect of backoff factor on the asymptotic throughput of the network. The commonly deployed binary exponential backoff (BEB) is close to optimum only for certain carrier-sensing systems like IEEE 802.11 distributed coordination function (DCF) request-to-send/clear-to-send (RTS/CTS) access scheme. For other systems such as ALOHA-like systems and IEEE 802.11 DCF basic access networks, BEB is far from optimum and the optimal backoff factor increases with the MPR capability. Moreover, our analysis shows that the maximum asymptotic throughput for both carrier-

sensing and non-carrier-sensing systems increases super-linearly with the MPR capability. This implies that the throughput per unit cost (e.g., bandwidth in CDMA systems or antenna in multi-antenna systems) increases as the MPR capability increases, providing a strong motivation for the use of MPR in future wireless networks. In addition to theoretical results, this thesis also proposes a joint MAC-PHY layer protocol that fully exploits the MPR capability of an IEEE 802.11-like wireless local area network.

摘要

沖突解決機制對于無線隨機接入網絡的性能至關重要。很多機制采用指數退避(EB)算法來調整發送概率以適應變化的網絡負荷。前人對于指數退避算法的研究大多基于傳統的單包接收模型。在這個模型當中，同一時刻只能有一個包被成功接收。然而，當物理層具有多包接收(MPR)能力時，媒體訪問控制層的行爲會和通常所認爲的有所不同。在本論文當中，我們分析指數退避算法基于多包接收模型的性能。在這個模型當中，多個包有可能同時被成功接收。本文的模型涵蓋了有限和無限用戶數目，並且適用于大多數現存的實際系統，即有載波監聽和無載波監聽的系統。我們的分析揭示了退避指數對于漸進吞吐量的影響。常用的二進制指數退避(BEB)算法在某些載波監聽系統，如 IEEE 802.11DCF RTS/CTS 接入系統中的性能非常接近最優。而對于其它像 ALOHA 類和 IEEE 802.11 DCF basic 接入系統中的性能和最優相差很遠，而且最佳的退避指數會隨 MPR 能力的增大而增大。除此之外，我們的分析顯示，對于載波監聽和非載波監聽系統，最大的漸進吞吐量隨 MPR 能

力的增大而增大。這就意味著單位成本獲得的吞吐量（例如：CDMA 系統的帶寬或者多天線系統的天線）隨 MPR 能力的增大而增大。這項發現爲在未來的無限網絡當中應用 MPR 提供了強有力的動機。除了理論上的結果，我們提出一個結合的 MAC-PHY 層協議來充分發掘一個 IEEE 802.11 類的無線局域網絡的 MPR 能力。

Acknowledgments

First of all, I would like to take this chance to express my sincere thanks to my supervisor Professor Ying Jun Zhang, for her patient and professional guidance in the past two years. She not only teaches me how to do research, but also helps me a lot in other ways. It is a great opportunity and pleasure to work towards my M.Phil. degree under her supervision.

I would also like to thank my co-supervisor Professor Soung Chang Liew, for numerous discussions and suggestions. He is really a role model to me.

I also want to express my thanks to all the members of the Wireless Networking Lab. We together create a friendly and cooperative research atmosphere, from which we all benefit.

Finally, I would like to give my hearty thanks to my parents, for their love, care and patience. I couldn't have achieved this without their support.

Table of Contents

List of Figures

List of Tables

Chapter 1
Introduction

1.1 Motivation

Collision-resolution schemes are a key component affecting network performance in a random-access wireless network. Core to a collision-resolution scheme is a backoff algorithm that determines how long a node should wait before retransmitting a packet after a collision. This backoff algorithm is an integral part of the whole system design and determines how well the system adapts to the ever changing traffic intensity in the network. Exponential backoff (EB), in which each collision causes the contention window to be multiplied by a constant factor, has been investigated in detail in the last few decades [1, 27-30]. In particular, binary exponential backoff (BEB), a special case of EB with backoff factor r equal to 2, is widely used in many practical systems because of its effectiveness and easy implementation.

Most previous work studying the behavior of EB was based on the traditional single-packet-reception model. However, with advanced physical-layer reception techniques, it is possible for the receiver to resolve multiple

simultaneously transmitted packets. For example, with CDMA [3] or multiple-antenna [4] techniques, it is no longer a physical constraint for the channel to accommodate only one ongoing transmission. Consequently, multiple packets can be received simultaneously without collisions. With multipacket reception (MPR) [2], collisions occur only when the number of simultaneously transmitted packets exceeds the maximum number of the simultaneous packets that the receiver can resolve. It is expected that, with improved MPR capability from the physical layer, the medium-access-control (MAC) layer will behave differently from what is commonly believed. Hence, we are motivated to establish a generic model to investigate the performance of EB with MPR in this thesis.

1.2 Related Work

The existing work on MPR can be broadly categorized into performance analysis and protocol design. With regard to performance analysis, Ghez, Verdu and Schwartz [6] were the first to analyze the stability properties of slotted Aloha with MPR capability in the late 1980s. Recently, Tong *et al.* have studied the impact of MPR-enabling signal-processing techniques on the throughput and design of random access protocols in [2]. However, to date, there has been little work that investigated the impact of MPR on the behavior of EB-based wireless networks. To the best of our knowledge, our analysis in [15] is the first to investigate the performance of EB with MPR capability in the literature. With regard to protocol design, Zhao and Tong proposed a centralized multiqueue service room MAC protocol (MQSR) in [7]. Building

upon a centralized scheduling scheme, their algorithm is not applicable to practical random-access networks. Hence, in [5] we proposed a distributed protocol to implement MPR in wireless LANs.

1.3 Our Contribution

Considering the wide adoption of EB in existing systems, we are motivated to (i) establish a universal model to study the fundamental performance of EB in a wireless network with MPR capability, and (ii) propose a distributed MAC-layer protocol and corresponding PHY-layer implementation to fully exploit the MPR capability in IEEE 802.11-like wireless local area networks (WLANs).

With regard to (i), we study wireless networks with and without carrier-sensing, assuming both finite and infinite populations. For a network with finite population, a Markov-chain model is adopted to derive the transmission probability, collision probability, and achievable throughput. To study the asymptotic behavior of EB, an infinite population model is further proposed. Based on the analytical results, we study in depth the impact of MPR on MAC behavior. Specifically, our results show that carrier-sensing and non-carrier-sensing systems share a number of common characteristics. For example, the asymptotic collision probability goes to $1/r$ (the reciprocal of the backoff factor) and the maximum achievable throughput increases super-linearly with the MPR capability in both cases. In addition, the commonly used BEB scheme does not necessarily yield the optimal network throughput in both systems with

MPR capability. For non-carrier-sensing systems, BEB is far from optimum and the optimal backoff factor increases with the MPR capability. For carrier-sensing systems, the optimal value of r depends heavily on the relative durations of idle, collision, and success slots. For example, BEB is close to optimum for IEEE 802.11 distributed coordination function (DCF) request-to-send/clear-to-send (RTS/CTS) access scheme, while it is far from optimum for IEEE DCF basic access scheme.

With regard to (ii), the proposed protocol is distributed and can be easily incorporated in an IEEE 802.11 DCF mode, which is currently a dominant WLAN standard. To the best of our knowledge, our work is the first to explore MPR in EB-based random-access networks both in theory and practice.

1.4 Organization of the Thesis

This thesis is organized as follows:

In Chapter 2, we introduce the system model and the underlying EB mechanism. In Chapter 3, we derive the expressions of transmission probability and collision probability, applying to both carrier-sensing and non-carrier-sensing networks. The convergence of transmission probability, collision probability, and the average attempt rate as the population size goes to infinity is also studied in this chapter. The throughput expression for non-carrier-sensing networks is derived in Chapter 4. Based on the throughput expression, we demonstrate how to adjust the backoff factor r to maximize the achievable throughput. In addition, an infinite population model is presented to analyze

the asymptotic behavior of EB. The performance of EB with MPR for carrier-sensing systems is studied in Chapter 5. Chapter 6 presents a MAC-PHY protocol to realize MPR in IEEE 802.11 WLANs. Chapter 7 discusses extensions of our analysis to a general MPR collision model. Finally, Chapter 8 concludes the thesis.

Chapter 2
Background Overview

2.1.1 Traditional Wireless Networks

2.1.1.1 Slotted ALOHA

ALOHA [16-20] was a pioneering computer networking system developed at the University of Hawaii. The ALOHA protocol is a MAC protocol for LAN networks with broadcast topology. The basic idea of this protocol is that whenever you have a packet to send, send it at the beginning of the next slot. If the packet collides with other packets, try sending it later. This scheme is very simple and robust. It is well know that the maximum achievable throughput is 0.368, twice that of pure ALOHA.

2.1.1.2 IEEE 802.11 DCF

WLANs have received much attention these years both from academic and the industry fields. The IEEE 802.11 [10, 21-26] standard defines the MAC and PHY layers for WLANs. The 802.11 standard works in two modes, one is called infrastructure mode, and the other is called ad hoc mode. In the

infrastructure mode, all communication goes through the access point (AP), while in the ad hoc mode, the stations just send to one another directly without the need of AP.

Two types of fundamental access mechanism are defined in the standard. One is called distributed coordination function (DCF), which is a random access scheme based on CSMA/CA (Carrier Sensing Multiple Access with Collision Avoidance) and does not use any kind of central control. The other one is called point coordination function (PCF), which is a centralized MAC scheme able to offer collision free services. All implementations must support DCF but PCF is optional, and most commercial products only implement DCF. Two access schemes are defined in the IEEE 802.11 DCF, basic access scheme and RTS/CTS access scheme. They all employ BEB as their collision resolution algorithm.

2.2 Exponential Backoff

2.2.1 Introduction

As mentioned earlier in Chapter 1, whenever the number of simultaneous transmissions exceeds the channel's MPR capability, collision happens and the packets involved are garbled. Therefore, once a collision occurs, a collision resolution scheme is needed for the colliding stations to optimally schedule retransmissions for the colliding packets.

One of the most widely used collision resolution protocols is the binary exponential backoff scheme, which is being included as part of the MAC

specifications in Ethernet [9] and IEEE 802.11 standards. In this thesis, we explore a general form of exponential backoff with arbitrary backoff factor r larger than one. BEB is a special case of the general EB with $r=2$.

2.2.2 Algorithm

The EB algorithm works as follows. Initially, any station with packets to transmit sets a backoff timer by randomly selecting an integer from 0 to W_0-1, where the integer W_0 denotes the minimum contention window size. The backoff timer is decreased by one following each backoff slot, which could be of variable length, depending on the type of system in use and the channel activity in the same slot. The station transmits a packet in its queue when the backoff timer reaches zero. Every time the transmission is unsuccessful, the contention window of the station will be multiplied by the backoff factor r. After i successive failed retransmissions, the number of backoff slots, D_i, for which the station will wait before the $i+1$ retransmission attempt, is of the following distribution [11]:

$$\Pr\{D_i = k\} = \begin{cases} \dfrac{I_i + 1 - F_i}{I_i(I_i+1)}, & k = 0, 1, \cdots, I_i - 1 \\ \dfrac{F_i}{I_i+1}, & k = I_i \end{cases} \tag{1}$$

where $I_i = \lfloor r^i W_0 \rfloor$ and $F_i = r^i W_0 - I_i$. Once a transmission is successful, the contention window of that station is reset to W_0.

According to the descriptions above, it is easy to see that a larger contention window results in a smaller transmission probability. The basic idea of EB is

intuitively explained as follows. In random access networks, a collision implies probable overloading of the channel. Hence, enlarging the contention window size of the colliding stations reduces their transmission probability, and the overall load on the channel is also reduced as a result. The EB thus serves as the feedback mechanism to prevent overloading of the channel.

2.2.3 Assumptions

A number of previous investigations in this area focus on the stability issues of EB. Interested readers are referred to [11] for a more detailed literature survey. Assuming EB stability (see next chapter for elaboration of our definition of stability), we perform a careful study of the impact of MPR on the performance of EB.

In order to focus on the effect of MPR on EB, we assume that the channel is error free in the sense that all packet losses are due to collisions. This assumption is widely adopted in the literature to simplify analysis and at the same time provide reasonable results. Nonetheless, our work can be easily extended to include the effect of random channel error by incorporating the packet error rate into the general MPR collision model introduced in Chapter 7.

2.3 System Description

2.3.1 MPR Capability

In this thesis, we investigate a fully connected random access network with a total of N mobile stations operating under saturated condition. Throughout the thesis, except in Chapter 7, we assume that the channel has the capability to

accommodate up to M simultaneous transmissions. More specifically, this means that the packets can be received correctly whenever the number of simultaneous transmissions is not larger than M. When more than M stations contend for the channel at the same time, no packet can be decoded. We refer to M as MPR capability hereafter. A more general form of MPR, in which packet receptions probabilistically depend on the number of simultaneous transmissions, will be discussed in Chapter 7.

2.3.2 Backoff Slot

The systems we consider in this thesis are time slotted and transmissions start only at the beginning of a slot. The transmission probability in each slot is governed by EB. The backoff timer at each station decreases by one after each slot. Note that the length of a slot is not necessarily fixed and may vary under different contexts. We refer to this variable-length slot as *backoff slot* hereafter. The length of a backoff slot depends on the contention outcome (refer to as *channel status* here) in that slot. It is an idle slot if nobody transmits; it is collided slot if more than M stations transmits; and it is a successful slot if the number of transmitting stations is anywhere from 1 to M. The durations of the corresponding backoff slots are T_i, T_c or T_s respectively. In this sense, the duration of a backoff slot is the variable time interval between two consecutive backoff timer decrements.

2.3.3 Carrier-sensing and Non-carrier-sensing Systems

To establish a general framework for the theoretical analysis of EB with MPR, we investigate its performance in both *carrier-sensing* and *non-carrier-sensing* slotted systems. The systems we study in this thesis cover most of the practical systems we encounter in real life. The methodology used in our analysis can be easily applied to other types of systems. For non-carrier-sensing systems like ALOHA networks, the stations are not aware of the channel status and therefore the duration of a backoff slot is always equal to a constant T_{slot}. That is, $T_i = T_c = T_s = T_{slot}$ in this case. On the other hand, for carrier-sensing systems, such as IEEE 802.11 DCF, the stations distinguish between various types of channel status, and the durations of the different types of slots may not be the same.

Chapter 3
Multipacket Reception in WLAN

Before we move on to the analysis of EB for carrier-sensing and non-carrier-sensing systems, it is better to present a big picture of what MPR is and how it works in practice. As an example, we propose a MAC protocol along with a physical layer implementation to support MPR for the widely adopted IEEE 802.11 WLANs. Our proposed MPR protocol is based on the IEEE 802.11 DCF RTS/CTS access scheme. We employ BEB as the underlying collision resolution scheme in the MPR MAC protocol. The reason why BEB is used will be explained later in the following chapters. We briefly describe the MPR MAC protocol and the PHY implementation in this chapter. The reader is referred to [5] for more details. The system configuration is depicted in Fig. 12. The AP is mounted with M antennas, while each client station has one antenna only. Again, we assume the network is fully connected for simplicity.

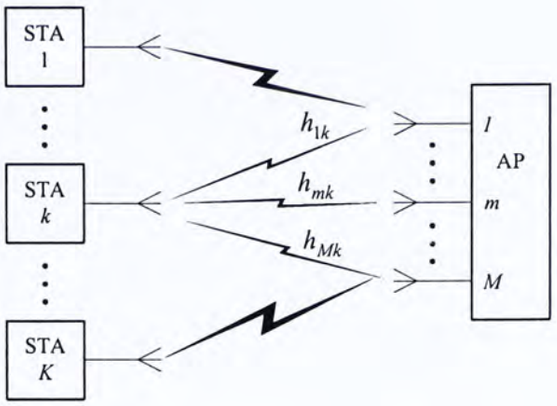

Figure 1 System model used for MPR.

3.1 MAC Protocol Description

The proposed protocol follows the IEEE 802.11 DCF RTS/CTS access mechanism closely, with an extension to support MPR. We consider the MAC protocol in this subsection. For simplicity, we consider a fully connected BSS with an AP and N associated client stations. We assume that the AP is the only station in the BSS with the capability to receive up to M ($M \geq 1$) packets simultaneously.

Figure 13 illustrates the protocol operation. A station with a packet to transmit first sends an RTS frame to the AP. In our MPR MAC model, when multiple stations transmit RTS frames at the same time, the AP can successfully detect all the RTS frames if and only if the number of RTSs is not larger than M. When the number of transmitting stations exceeds M, collisions occur and the AP cannot decode any of the RTSs. The stations will retransmit their RTS frames after a backoff time period according to the original IEEE 802.11 protocol. When the AP detects the RTSs successfully, it responds, after a SIFS period, with a CTS frame that grants transmission permissions to all the

requesting stations. Then the transmitting stations will start transmitting DATA frames after a SIFS, and the AP will acknowledge the reception of the DATA frames by an ACK frame.

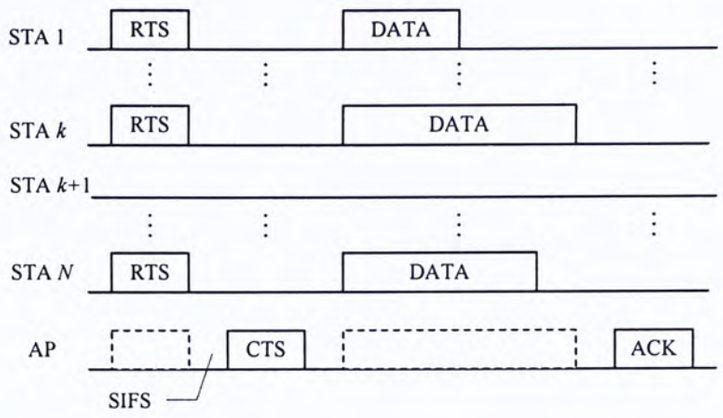

Figure 2 Time line example for the MPR MAC.

The formats of the RTS and Data frames are the same as those defined in 802.11, while the CTS and ACK frames have been modified to accommodate multiple transmitting stations for MPR. In particular, there are M receiver address fields in the CTS and ACK frames to identify up to M intended recipients.

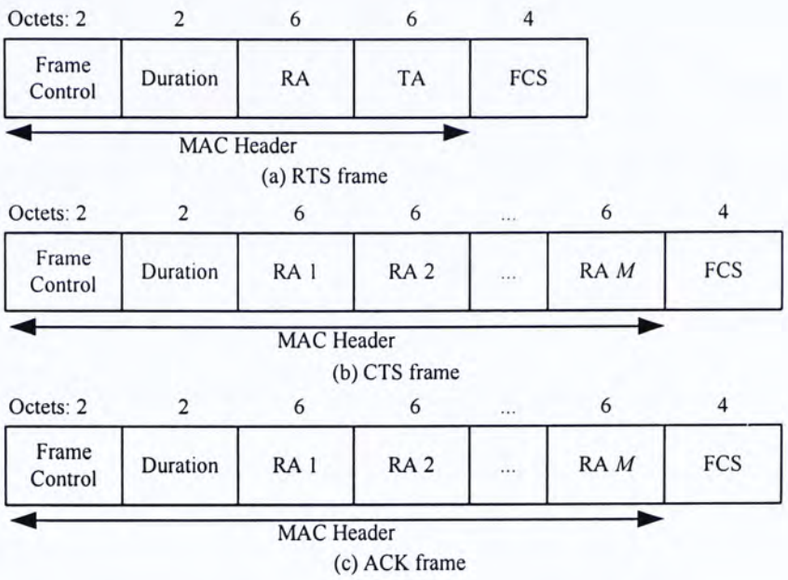

Figure 3 Formats of control frames for the MPR MAC.

As described above, our MPR MAC is very similar to the original IEEE 802.11 MAC. In fact, to maintain this similarity in the MAC layer, the challenge is pushed down to the physical layer. For example, in the proposed MPR MAC, multiple RTS packets may be transmitted at the same time and the AP is responsible to decode all the RTSs as long as the number of simultaneously transmitted RTSs is not larger than M. However, this is no easy job. Since the AP has no priori knowledge of who the senders are as well as the CSI on the corresponding links, MUD techniques such as Zero Forcing (ZF) and Minimum Mean Squared Error (MMSE) cannot be directly applied. To tackle these problems, we introduce the physical layer techniques in next subsection.

3.2 Physical Layer Methodology

In this subsection, we propose a mechanism to implement MPR in IEEE 802.11. The basic idea is as follows. RTS packets are typically transmitted at a lower data rate than the data packets in IEEE 802.11. This setting matches well with blind detection algorithms, such as Constant Modulus (CM) or Finite Alphabet (FA), with which separation of multiple RTS packets can be achieved with reasonable computational complexity [4, 13]. In our proposed system, an FA-based blind detection scheme is applied to decode the RTS packets that are simultaneously transmitted from K stations for $K \leq M$. Upon successfully decoding the RTS packets, the AP can then identify the senders of the packets. Training sequences, to be transmitted in the preamble of the data packets, are then allocated to these users to facilitate channel estimation during the data transmission phase. Since the K stations will transmit their data packets at the same time, their training sequences should be mutually orthogonal. In our system, no more than M simultaneous transmissions are allowed, since there are M antennas at the AP. Therefore, a total of M orthogonal sequences are required to be predefined and made known to all stations in the BSS. The sequence allocation decision is sent to the users via the CTS packet.

During the data transmission phase, CSI is estimated from the orthogonal training sequences that are transmitted in the preamble of the data packets. With the estimated CSI, various MUD techniques can be applied to separate the multiple data packets at the AP. Using coherent detection, data packets can

be transmitted at a much higher rate than the RTS packets without involving excessive computational complexity.

The details of the PHY realization of MPR are presented in the following subsections.

3.2.1 Blind RTS Separation

Assume that the delay spread is smaller than the symbol duration, and hence the effect of the channel is approximated by complex amplitude scaling. Let $h_{m,k}$ denote the channel coefficient from user k to the m^{th} receive antenna, and $x_k(n)$ denote the symbol transmitted by user k over symbol duration n. The received signals can then be written as

$$\mathbf{y}(n) = \left[y_1(n), y_2(n), \cdots, y_M(n)\right]^T = \mathbf{H}\mathbf{x}(n) + \mathbf{w}(n) \tag{33}$$

where

$$\mathbf{H} = \begin{bmatrix} h_{1,1} & h_{1,2} & \cdots & h_{1,K} \\ h_{2,1} & h_{2,2} & \cdots & h_{2,K} \\ \vdots & \vdots & \ddots & \vdots \\ h_{M,1} & h_{M,2} & \cdots & h_{M,K} \end{bmatrix}, \tag{34}$$

$$\mathbf{x}(n) = \left[x_1(n), x_2(n), \cdots, x_K(n)\right]^T, \tag{35}$$

and $\mathbf{w}(n)$ is the additive white noise received in the nth symbol duration. In indoor environment, large angular spread is typically observed at the AP. Therefore, the entries in the channel matrix $\mathbf{H}$ are modelled as i.i.d. complex Gaussian random variables.

Assuming that the channel is constant over an RTS packet, which is composed of N symbol periods, we obtain the following block formulation of the data

$$\mathbf{Y} = \mathbf{HX} + \mathbf{W} \tag{36}$$

where $\mathbf{Y} = [\mathbf{y}(1), \mathbf{y}(2), \cdots \mathbf{y}(N)]$, $\mathbf{X} = [\mathbf{x}(1), \mathbf{x}(2), \cdots \mathbf{x}(N)]$, and $\mathbf{W} = [\mathbf{w}(1), \mathbf{w}(2), \cdots \mathbf{w}(N)]$. The problem to be addressed here is the estimation of the number of sources K, the channel matrix $\mathbf{H}$, and the symbol matrix $\mathbf{X}$, given the array output $\mathbf{Y}$.

3.2.1.1 Estimation of the number of sources *K*

For an easy start, we ignore the white noise for the moment and have $\mathbf{Y} = \mathbf{HX}$. The rank of $\mathbf{H}$ is equal to K if $K \leq M$. Likewise, $\mathbf{X}$ is full-row-rank when N is much larger than K. Consequently, we have $rank(\mathbf{Y}) = K$ and K is equal to the number of nonzero singular values. With white noise added to the data, K can be estimated from the number of singular values of $\mathbf{Y}$ that are significantly larger than zero.

3.2.1.2 Estimation of X and H

The maximum-likelihood estimator yields the following separable least-squares minimization problem [4]

$$\min_{\mathbf{H},\mathbf{X}\in\Omega} \|\mathbf{Y} - \mathbf{HX}\|_F^2 \tag{37}$$

where Ω is the finite alphabet to which the elements of $\mathbf{X}$ belong, and $\|\cdot\|_F^2$ is the Frobenius norm. The minimization of (37) can be carried out in two steps. First, we minimize (37) with respect to $\mathbf{H}$ and obtain

$$\hat{\mathbf{H}} = \mathbf{YX}^{+} = \mathbf{YX}^{H}\left(\mathbf{XX}^{H}\right)^{-1}, \tag{38}$$

where $(\cdot)^+$ is the pseudo-inverse of a matrix. Substituting $\hat{\mathbf{H}}$ back into (37), we obtain a new criterion, which is a function of $\mathbf{X}$ only:

$$\min_{\mathbf{X}\in\Omega} \left\| \mathbf{Y}\mathbf{P}^{\perp}_{\mathbf{X}^H} \right\|_F^2, \tag{39}$$

where $\mathbf{P}^{\perp}_{\mathbf{X}^H} = \mathbf{I} - \mathbf{X}^H \left(\mathbf{X}\mathbf{X}^H\right)^{-1} \mathbf{X}$, and $\mathbf{I}$ is the identity matrix. The global minimum of (39) can be obtained by enumerating over all possible choices of $\mathbf{X}$. Reduced-complexity iterative algorithms that solve (39) iteratively such as ILSP and ILSE were introduced in [14]. Not being one of the foci of this thesis, the details of ILSP and ILSE are not covered here. Interested readers are referred to [14] and the references therein.

3.2.2 Data Packet Detection

After successfully decoding the RTS packets at the AP, the orthogonal training sequences are allocated to the requesting stations through the CTS packet. Given the orthogonal training sequences, the CSI in the data transmission phase can be estimated more accurately. We omit the index n in this subsection, since the following processing is on a per-symbol basis. In a given symbol period, the received vector is

$$\mathbf{y} = \sum_{k=1}^{K} \mathbf{h}_k x_k + \mathbf{w} = \mathbf{H}\mathbf{x} + \mathbf{w}, \tag{40}$$

where $\mathbf{h}_k = \left[h_{1,k}, h_{2,k}, \cdots, h_{M,k} \right]^T$. To separate the signals from multiple users, various MUD techniques have been proposed in the literature. For example, the ZF (Zero Forcing) receiver is one of the most popular linear detectors. It

multiplies the received vector by a decorrelation matrix $\mathbf{H}^{+}$, and the decision statistics become

$$\mathbf{r}^{ZF} = \mathbf{H}^{+}\mathbf{y} = \mathbf{x} + \mathbf{H}^{+}\mathbf{w}. \tag{41}$$

In contrast, the MMSE (Minimum Mean Square Error) receiver takes into account both the co-channel interference and the noise term. Such a receiver is an optimal linear detector in the sense of maximizing the SINR (Signal to Interference and Noise Ratio). The decision statistics are formulated by

$$\mathbf{r}^{MMSE} = \left(\mathbf{H}\mathbf{H}^{H} + \sigma^{2}\mathbf{I}\right)^{-1}\mathbf{H}^{H}\mathbf{y}. \tag{42}$$

Given the decision statistics, an estimate of x_k can be obtained by feeding the k^{th} element of $\mathbf{r}^{ZF}$ or $\mathbf{r}^{MMSE}$ into a quantizer.

Chapter 4 Exponential Backoff with MPR

The model we use in the following analysis is commonly known as the time-slotted model. This model assumes that the time axis is divided into slots, which are not necessarily of the same length. There are N fully connected stations individually operating in a saturated mode, giving the stations a constant supply of packets available for transmission. All packet transmissions are of the same length and well synchronized, starting at the beginning of each slot. After each transmission, we assume the transmitting stations have a means to discover the result of the transmission, i.e., success or failure. As mentioned in the previous chapter, we assume that all packet failures are due to collisions for easy discussion. The results derived in this chapter are system independent and therefore applicable to both carrier-sensing and non-carrier-sensing systems. In some sense, our analysis in this chapter can be regarded as a generalization of [11] applied to the MPR framework.

4.1 Analytical Model

4.1.1 Markov Model

We use an infinite-state Markov chain, as shown in Fig. 1, to model the operation of EB with no retry limit at a station. The reason for the lack of a retry limit is that it is theoretically more interesting to look at the limiting case when the retry limit is infinitely large. Besides, by taking out the retry limit, we have the advantage of having fewer variables so that clearer relations between the more interesting parameters can be manifested. Having said this, we note that the analysis in our thesis can be easily extended to the case where there is a retry limit. The state in the Markov chain in Fig. 1 is the backoff stage, which is also equal to the number of retransmissions experienced by the station. Therefore, the contention window size is $W_i = r^i W_0$ when the station is in state i. In our model, we assume that the collision probability of each transmission attempt is equal to a constant p_c, no matter what state the station is currently in. This assumption is accurate as long as N is large enough [12]. We also assume that with the use of EB at all stations, the stations will finally reach a steady state in which the distribution of the backoff stages of the stations becomes stationary. So we define "stability" as the capability of EB to adapt to the varying traffic condition and finally to bring the system into a steady state.

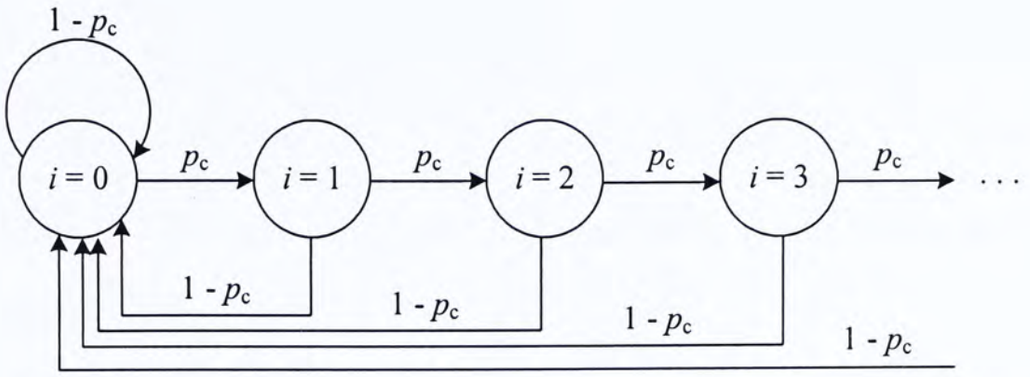

Figure 4 Markov chain model for the backoff stage.

4.1.2 Relations between p_t and p_c

Let B_k denote the k-th state in the Markov chain, then it can be easily figured out that the non null transition probabilities are

$$\begin{cases} p_{i,i+1} = \Pr\{B_{k+1} = i+1 \mid B_k = i\} = p_c \\ p_{i,0} = \Pr\{B_{k+1} = 0 \mid B_k = i\} = 1 - p_c \end{cases}, \quad i = 0, 1, \cdots . \tag{2}$$

Then the frequency that state i is visited in the steady state can be obtained as follows:

$$P_i = \Pr\{B_k = i\} = (1 - p_c) p_c^i . \tag{3}$$

A station has to wait for D_i slots before a packet can be transmitted. So, on average, the station stays in state i for

$$\overline{d_i} = E[D_i + 1] = \frac{W_i + 1}{2} \tag{4}$$

slots before it moves to the next state. Thus, in the steady state, the probability that a station is in state i at a given time is given by

$$S_i = \frac{P_i \overline{d_i}}{\sum_{k=0}^{\infty} P_k \overline{d_k}} = \frac{(1-p_c)p_c^i(1-rp_c)(W_i+1)}{W_0(1-p_c)+1-rp_c}. \quad (5)$$

Here, $rp_c < 1$ is a necessary condition for the steady state to be reachable. Otherwise, the summation

$$\sum_{k=0}^{\infty} P_k \overline{d_k} = \frac{W_0(1-p_c)+1-rp_c}{2(1-rp_c)} \quad (6)$$

does not exist.

It is generally agreed that EB can be modelled reasonably well by a process in which each station attempts to transmit in each backoff slot independently and identically with a probability. Let p_t denote that transmission probability of a station in an arbitrary backoff slot. Noting the fact that a station will transmit only when the backoff timer counts down to 0, we have

$$p_t = \sum_{i=0}^{\infty} s_{i,0}, \quad (7)$$

where $s_{i,0}$ is the probability that a station is in state i and the backoff timer is 0, and can be expressed as

$$s_{i,0} = \frac{S_i}{\overline{d_i}} = \frac{2(1-p_c)p_c^i(1-rp_c)}{W_0(1-p_c)+1-rp_c}. \quad (8)$$

Thus, we get

$$p_t = \frac{2(1-rp_c)}{W_0(1-p_c)+1-rp_c}. \tag{9}$$

Interested reader can refer to [11] for detailed derivation of p_t. It is somewhat intriguing that relationship (9) applies to both MPR and non-MPR systems. The key difference between the systems is from the relationship in the next paragraph.

In the steady state, the probability of a transmitted packet suffering collision is equal to the probability that the number of simultaneous transmissions from the other $N-1$ stations is M or more. Thus, we have the following relation:

$$p_c = 1-\sum_{k=0}^{M-1}\binom{N-1}{k} p_t^k (1-p_t)^{N-k-1}. \tag{10}$$

From (9) and (10), we can solve for p_c and p_t, given N, M, r and W_0. The curves determined by (9) and (10) are plotted in Fig. 2. This unique intersection represents the roots p_c and p_t of (9) and (10), which could be calculated numerically. From the figure, we can also see that as N increases, p_t and p_c converge to 0 and 0.5 (i.e., $1/r$ when $r=2$) respectively, regardless of M. This observation is proved analytically in Chapter 3.3.

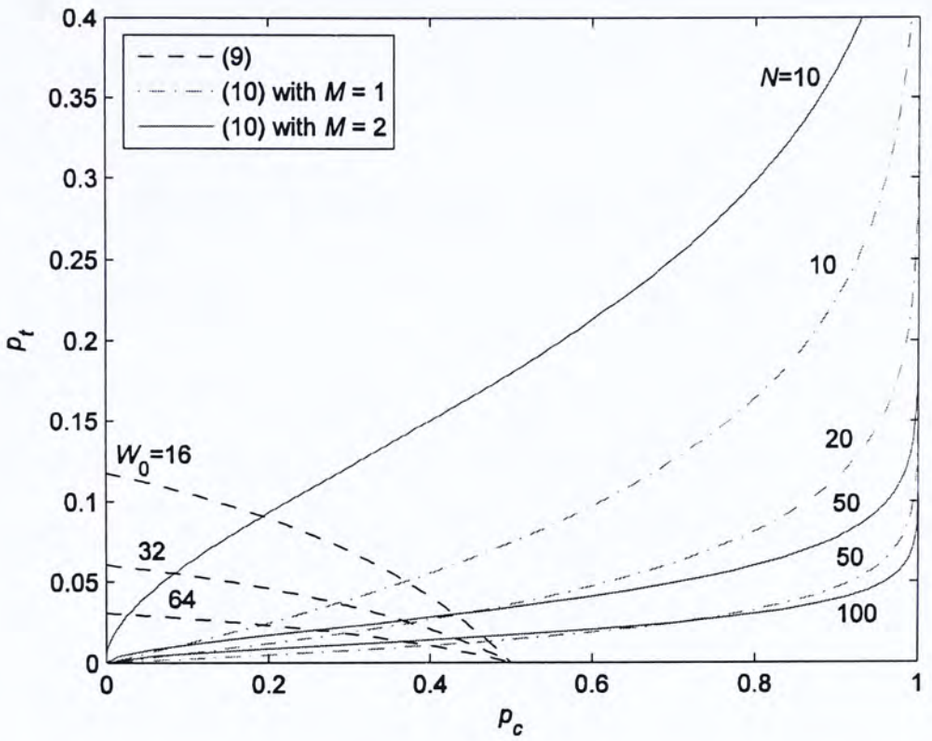

Figure 5 Plots of p_t as a function of p_c when $r = 2$; dashed lines: p_t in (9), dotted lines: p_t in (10) with $M = 1$, $r = 2$, solid lines: p_t in (10) with $M = 2$.

4.2 Simulation Settings

The simulator we develop realizes the EB algorithm described in Chapter 2.2 along with those assumptions mentioned earlier. The simulator is written in C++ and developed under Visual C++ 6.0 IDE. The data are collected by running 5,000,000 rounds after 1,000,000 rounds of warm up, in the same way as in [11]. The backoff factor r we use in the simulation is 2, so the general EB reduces to BEB and the minimum contention window sizes we choose are $W_0 = 16$, 32, and 64, conforming to the IEEE 802.11 specification for different PHY layers. We only show the simulation results when $M = 1$ and 2. The curves for other M can be inferred from these two special cases.

4.3 Asymptotic Behavior of Exponential Backoff

4.3.1 Convergence of p_t and p_c

First, it is not difficult to see that $\lim_{N\to\infty} p_t = 0$ is necessary for the system to reach a steady state, which is our initial assumption. Suppose p_t converges to some nonzero value, then Np_t, the number of average transmission attempts in a backoff slot, approaches infinity as N goes to infinity. This implies that the collision probability p_c equals to 1 for a system with limited MPR capability, which does not satisfy the necessary condition $p_c < 1/r$ for the system to be able to reach the steady state. Hence, p_t converges to zero as N goes to infinity. Taking the limit of (9) on both sides, we should have

$$\lim_{N\to\infty} p_t = \lim_{N\to\infty} \frac{2(1-rp_c)}{W_0(1-p_c)+1-rp_c} = 0$$

which implies

$$\lim_{N\to\infty} 2(1-rp_c) = 0 .$$

Therefore, we have

$$\lim_{N\to\infty} p_c = \frac{1}{r} \quad \text{for finite } M . \tag{11}$$

From (11), we conclude that p_c converges to $1/r$ regardless of M as N goes to infinity. We plot the analytical results of p_c, obtained by calculating (9) and (10) numerically, as lines in Fig. 3.

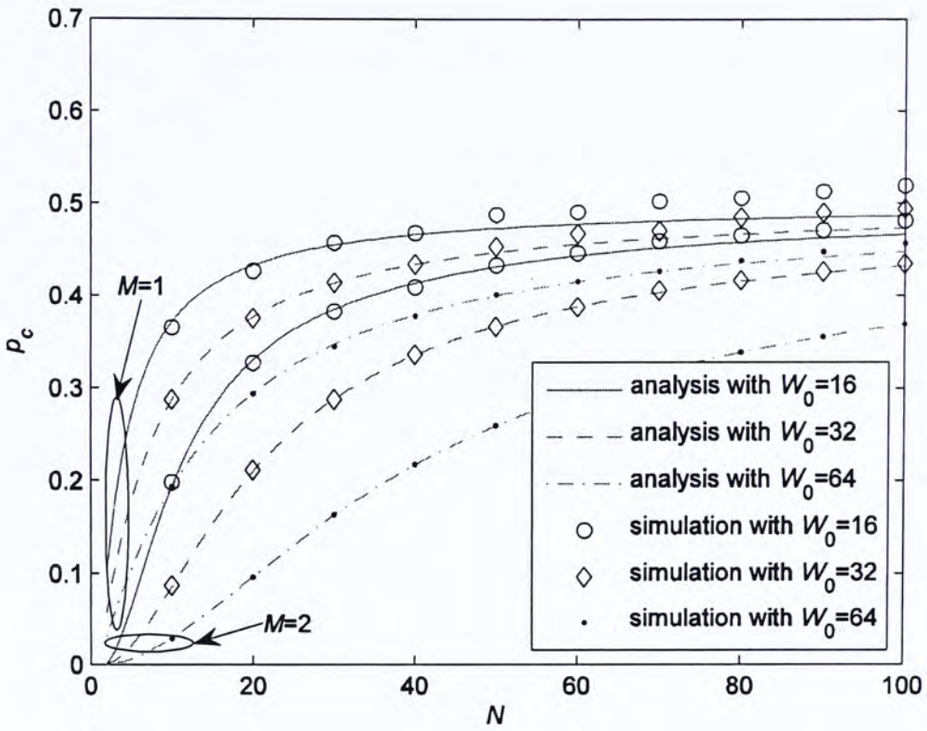

Figure 6 Plots of p_c versus N when $r = 2$; lines are analytical results calculated from (9) and (10), markers are simulation results.

In Fig. 3, both the curves for $M = 1$ and $M = 2$ converge to 0.5 (i.e., $1/r$ since $r = 2$). We can also see from Fig. 3 that the simulation results match well with the analytical results, which supports our conclusion in (11). It is obvious in the figure that as N increases, p_c increases to $1/r$ more slowly for $M = 2$ than for $M = 1$. The effect of W_0 on p_c is also observed in this figure. For any given N, the larger the W_0, the smaller the p_c. These results are self-evident since when the MPR capability or the minimum contention window size is increased, it is less likely for a station to collide with others.

4.3.2 Convergence of Np_t

We have shown that $\lim_{N\to\infty} p_t = 0$ in the discussions above. From Fig. 4, we can see that, with the same M, Np_t converges to a constant. This observation implies that the average number of transmission attempts in a backoff slot approaches a constant as N becomes infinitely large. This fact serves as a basis for the infinite population model to be presented in the following chapter. As a special case when $M = 1$ Kwak *et al.* showed in [11] that

$$\lim_{N\to\infty} Np_t = \ln\frac{r}{r-1}. \tag{12}$$

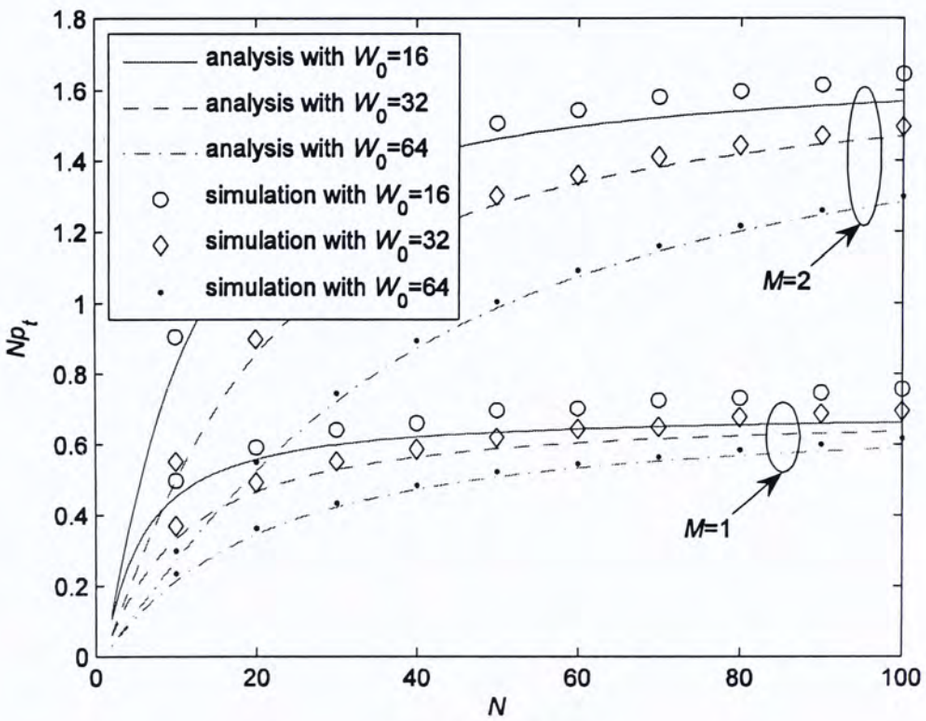

Figure 7 Plots of Np_t versus N when $r = 2$; lines are analytical results calculated from (9) and (10), markers are simulation results.

It is clear that $\lim_{N\to\infty} Np_t$ is a function of r and extensive numerical and simulation results show that this fact also holds for various M. We will demonstrate how to predict $\lim_{N\to\infty} Np_t$ numerically by using the infinite population model later in the next chapter.

Chapter 5
Non-carrier-sensing System

5.1 Performance Analysis

5.1.1 Throughput Derivation

With the common results derived in Chapter 3, we analyze the performance of EB for non-carrier-sensing system in this chapter. Recall that the main characteristic for non-carrier-sensing system is the constant backoff slot of length T_{slot}. Let P_{tr} be the probability that there is at least one transmission in a backoff slot. Then,

$$P_{tr} = 1-(1-p_t)^N . \tag{13}$$

Let P_{tk} denote the probability that k packets are transmitted simultaneously in a backoff slot, with the condition that there is at least one transmission. Since each station transmits its packet independently in a given backoff slot, the probability P_{tk} is calculated as

$$P_{tk} = \binom{N}{k} p_t^k (1-p_t)^{N-k} \Big/ P_{tr} . \tag{14}$$

The throughput of the network is

$$S = \frac{E[\text{payload information bits transmitted in a backoff slot}]}{E[\text{length of a backoff slot}]}$$
$$= \frac{\sum_{k=1}^{M} kP_{tk}P_{tr}L}{T_{slot}} \tag{15}$$

where L is the payload length of the packets in unit of bits. Define

$$S^* = T_{slot}S/L = \sum_{k=1}^{M} k\binom{N}{k} p_t^k (1-p_t)^{N-k} \tag{16}$$

which is unitless and conforms to the definition of the "normalized throughput" used in [11] for $M = 1$. Differing from the value of S only by a constant factor, S^* will be used as the throughput performance metric later in this chapter to make comparison with the results in [11].

5.1.2 Throughput Analysis

A question for us is how the throughput behaves as M increases, given a fixed number of stations N. The analytical results obtained when $N = 50$ are plotted in Fig. 5. In this figure, it can be seen that the throughput increases with M when M is much smaller than N, and reaches the maximum as M approaches N. In addition, the maximum throughput decreases as W_0 increases. There are several reasons behind this. First, it is obvious that the maximum throughput is reached when $M = N$. In this case, there is no collision and all transmissions are successful. Therefore, the contention window size is always equal to W_0. It can be easily derived that the maximum throughput is equal to $2N/(W_0 + 1)$. This implies that the maximum throughput decreases monotonically with W_0 when N is fixed.

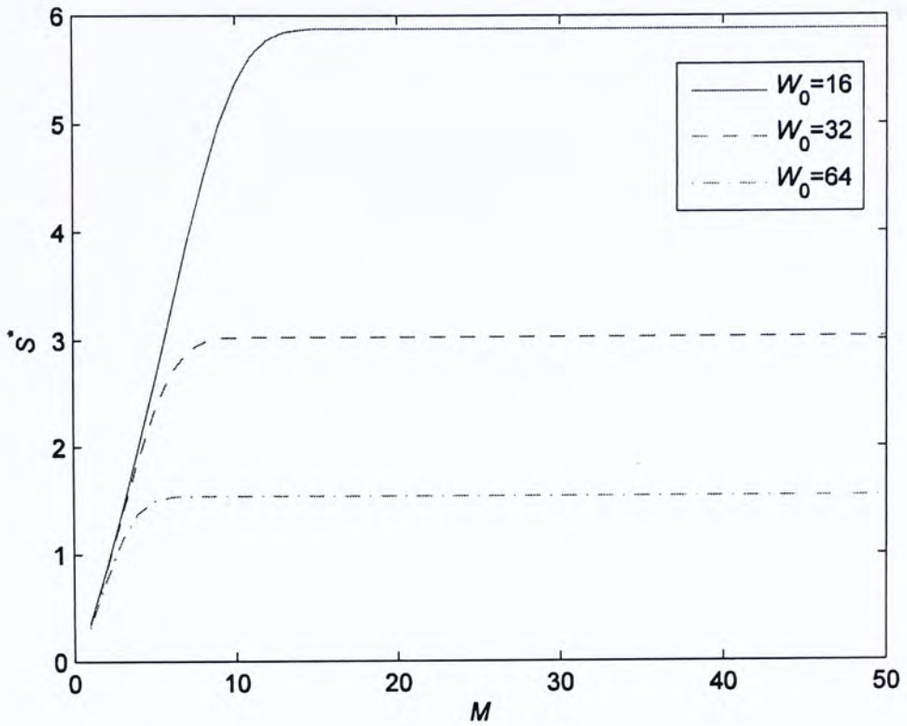

Figure 8 Throughput S^* versus M for non-carrier-sensing systems when $r = 2$ and $N = 50$.

In practice, MPR capability can be enhanced by increasing both hardware and computational costs. It is therefore worthwhile investigating the achievable throughput per unit cost in our system. As shown in Fig. 5, the throughputs become almost flat as M approaches N. Therefore, the normalized throughput (normalized by M) actually increases with M at first and then goes down as plotted in Fig. 6. The optimal point should be somewhere around the corner of the curve. While this is true for finite N, as we will see in the next subsection, the normalized throughput increases monotonically with M for infinite N.

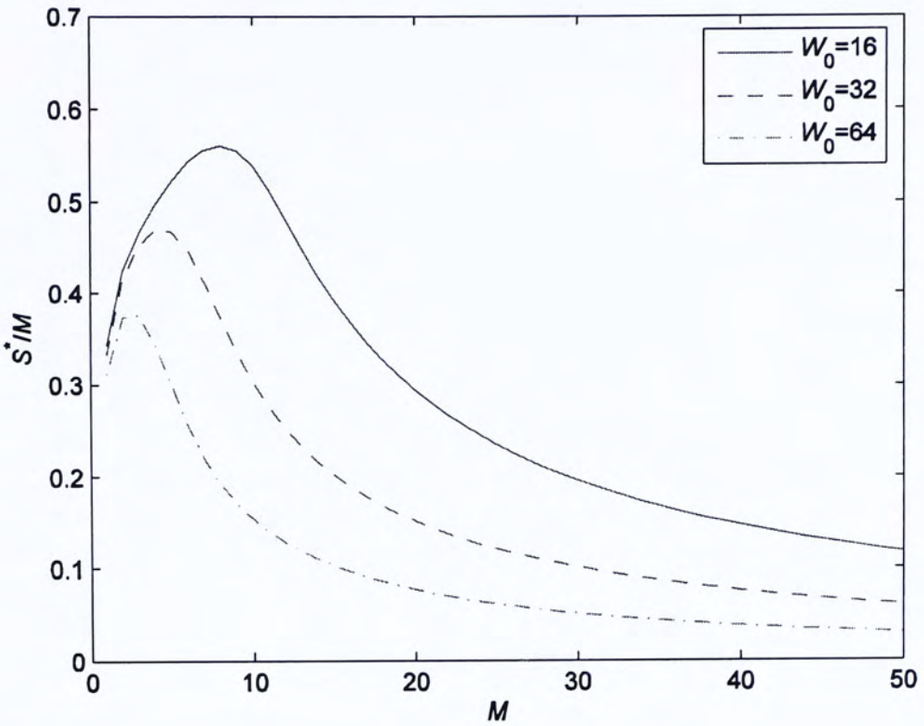

Figure 9 Normalized throughput S^*/M versus M for non-carrier-sensing systems when $r = 2$ and $N = 50$.

Similarly, the relation between throughput and r, given M, can also be obtained from (9), (10) and (16). Fig. 7 shows the throughput variation with different settings of r.

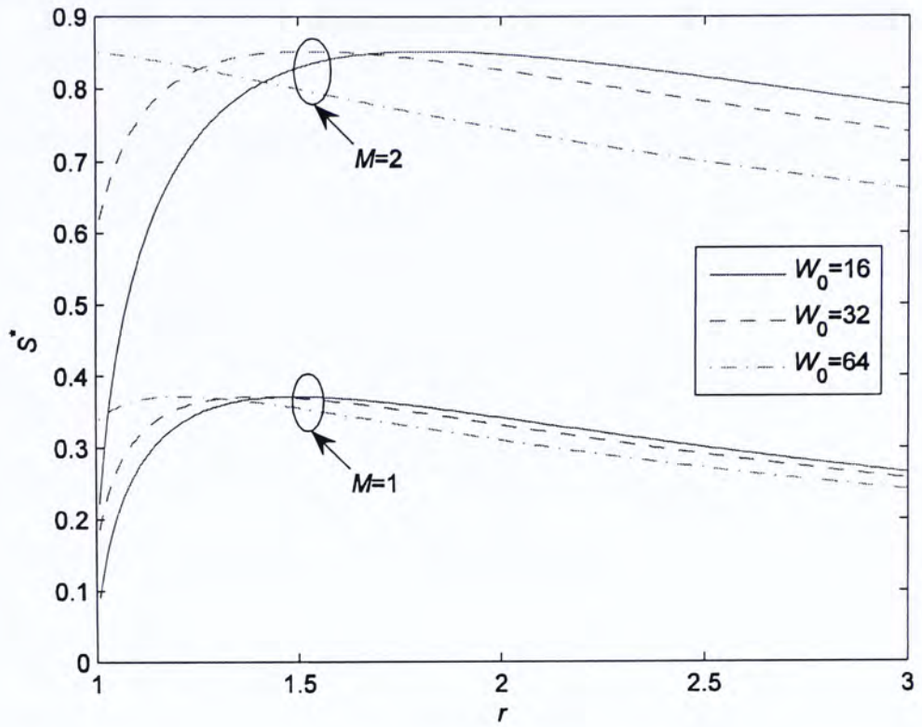

Figure 10 Throughput versus backoff factor *r* for non-carrier-sensing systems when $N = 50$.

From this figure, we can see that, given M, there exists an optimal value of r that maximizes the network throughput. This fact can be interpreted as follows. When r is increased, the collision probability is reduced. However, too much backoff causes the reduction of transmission probability at the same time. Thus, to maximize the throughput by calibrating the backoff factor r, we are indeed balancing between two opposing effects. One is letting the stations be more aggressive at the risk of higher collision probability and the other is letting them be conservative at the risk of wasting precious air time when nobody transmits at all. Mathematically, the optimal value of r that maximizes the throughput can be obtained by solving the equation

$$dS^*/dr = 0. \tag{17}$$

Another observation from this figure is that the commonly deployed BEB is not optimal because $r = 2$ does not achieve the maximum aggregate throughput. Similar conclusions also hold for the infinite population case and will be discussed in detail in the following subsections.

5.1.3 Convergence of S^*

We now analyze the asymptotic behavior of S^* in our MPR model. As described above, the throughput S^* can be obtained by solving (9), (10) and (16). From Fig. 8, we can see that the throughputs with the same M converge to the same constant as N increases, regardless of W_0. This phenomenon implies that no matter how crowded the network is, EB guarantees a nonzero limiting throughput. This limiting throughput depends only on the MPR capability of the channel and is insensitive to the settings of the initial minimum contention window size. In the next subsection, we will demonstrate how to predict this limiting throughput from the infinite-population model. As shown in Fig. 8, this limiting throughput increases as M increases, as expected.

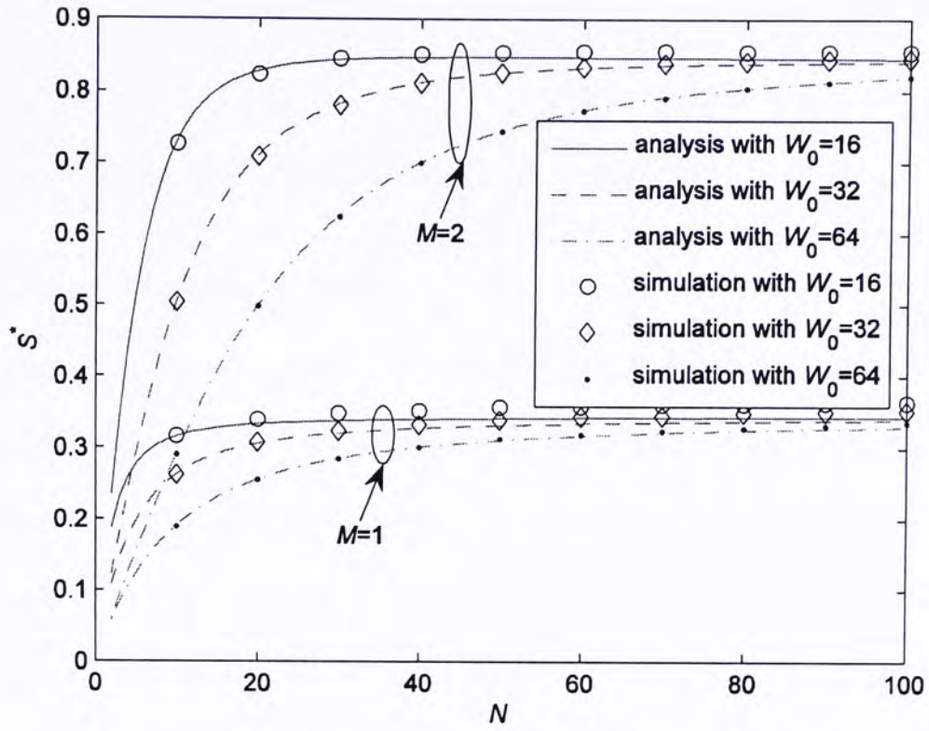

Figure 11 Plots of throughput S^* versus N for non-carrier-sensing systems when $r = 2$; lines are analytical results obtained numerically, markers are simulation results.

As a special case of our general MPR model when $M = 1$, Kwak *et al.* [11] proved that, under the traditional collision model, the network throughput S^* converges as the number of stations N goes to infinity as follows:

$$\lim_{N\to\infty} S^* = \frac{r-1}{r}\ln\frac{r}{r-1}. \tag{18}$$

As shown in (18), when $M = 1$, the asymptotic throughput is expressed as a function of r. The optimal r that maximizes the asymptotic throughput is given by [11]

$$r_{opt} = 1/(1-e^{-1}). \tag{19}$$

However, when M is larger than 1, it is difficult to express S^* as a closed-form function of r, so numerical methods are needed to find the optimal r.

5.2 Infinite Population Model

5.2.1 Attempt Rate

In the previous subsection, we studied EB and achievable throughput of wireless networks with MPR when the number of stations is finite and equal to N. The asymptotic performance when N approaches infinity can be obtained by setting N to be a very large number in the previously derived equations. However, this would make the numerical results difficult to obtain. In this subsection, we adopt an alternative infinite-population model to analyze the asymptotic performance of MPR. In this model, it is assumed that the number of stations N in the network is infinitely large and each station independently transmits in a backoff slot with the probability p_t. Recall that $\lim_{N\to\infty} p_t = 0$, while $\lim_{N\to\infty} Np_t$ is a constant. Therefore, the originally binomially distributed number of transmission attempts in a slot can be approximated by Poisson distribution:

$$\Pr\{X = n\} = \frac{\lambda^n}{n!} e^{-\lambda} \tag{20}$$

where the random variable X denotes the number of attempts in a slot and λ is the mean which can be expressed as

$$\lambda = \lim_{N\to\infty} Np_t . \tag{21}$$

In (11), we have shown that

$$\lim_{N\to\infty} p_c = \frac{1}{r}.$$

Meanwhile, from our infinite population model, we have

$$\lim_{N\to\infty} p_c = \Pr\{X \geq M\} = 1 - \Pr\{X \leq M-1\}. \tag{22}$$

Thus, from (11) and (22), we get the following equation

$$\Pr\{X \leq M-1\} = \sum_{k=0}^{M-1} \frac{\lambda^k}{k!} e^{-\lambda} = e^{-\lambda} \sum_{k=0}^{M-1} \frac{\lambda^k}{k!} = 1 - \frac{1}{r}. \tag{23}$$

This equation relates the attempt rate λ with the values of M and r, allowing easy calculation of λ from (23), given M and r.

5.2.2 Asymptotic Throughput of Non-carrier-sensing System

Finally, the asymptotic throughput is given by

$$\begin{aligned} \lim_{N\to\infty} S^* &= \sum_{k=1}^{M} k \Pr\{X = k\} = \lambda \sum_{k=0}^{M-1} \Pr\{X = k\} \\ &= \lambda \Pr\{X \leq M-1\} = \lambda(1 - \frac{1}{r}) \end{aligned} \tag{24}$$

Note that the asymptotic throughput is expressed by λ and r. Since λ is determined by M and r, the asymptotic throughput is indeed only a function of M and r.

Given r and M, we can calculate λ from (23). The asymptotic throughput is then obtained by substituting the value of λ into (24). Figure 9 is a plot of the asymptotic throughput versus r for various M. From this figure, we can see that the optimal r that maximizes the asymptotic throughput increases with M. This result seems somewhat counterintuitive, for it is generally believed that with a

larger M, r should be decreased to encourage the stations to be more aggressive. It is true that increasing r will reduce the number of attempts in a backoff slot, but on the other hand this will raise the success probability of an attempt. It is the weighting of these two effects that decides the optimal operating point of r. From the results, we can conclude that as M increases, the latter effect mentioned above dominates and in the end moves r to the right to achieve the maximum asymptotic throughput. Note that the asymptotic throughput decreases sharply when r moves from the r_{opt} to 1. On the other hand, the curve is somewhat flat when r is larger than the r_{opt}. Therefore, in order to avoid dramatic throughput degradation, it is not wise to operate r in the region between 1 and r_{opt}. Based on these observations, we argue that it is safer to set r large enough in non-carrier-sensing systems.

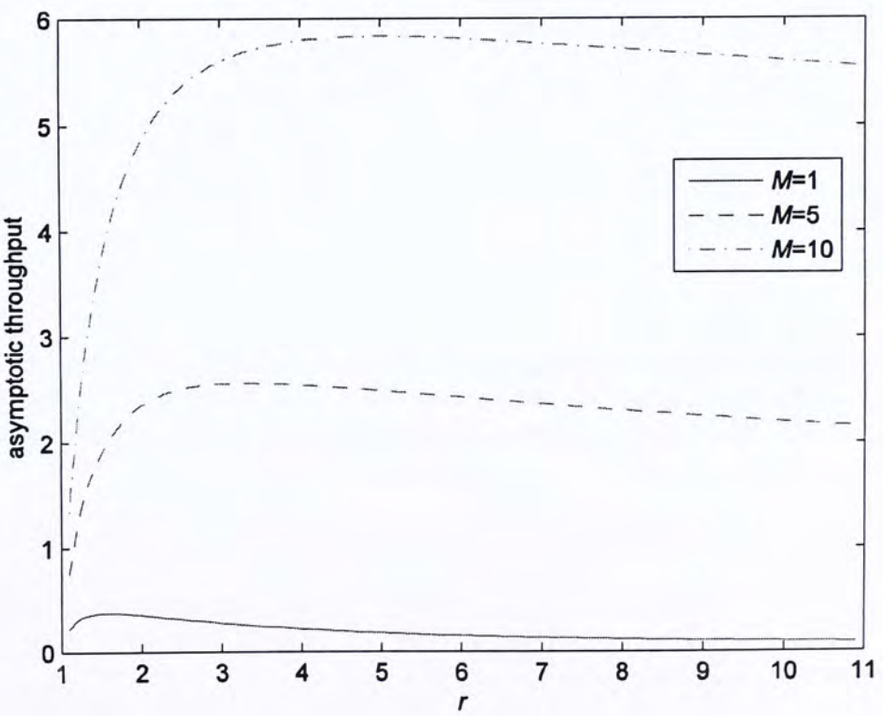

Figure 12 Asymptotic throughput versus r for non-carrier-sensing systems.

To see how well the commonly used BEB works, we plot the ratio of BEB's asymptotic throughput to the maximum achievable asymptotic throughput in Fig. 10. A direct conclusion from this figure is that BEB ($r = 2$) is far from optimum. For example, when $M = 10$ BEB only achieves about 80 percent of the maximum asymptotic throughput.

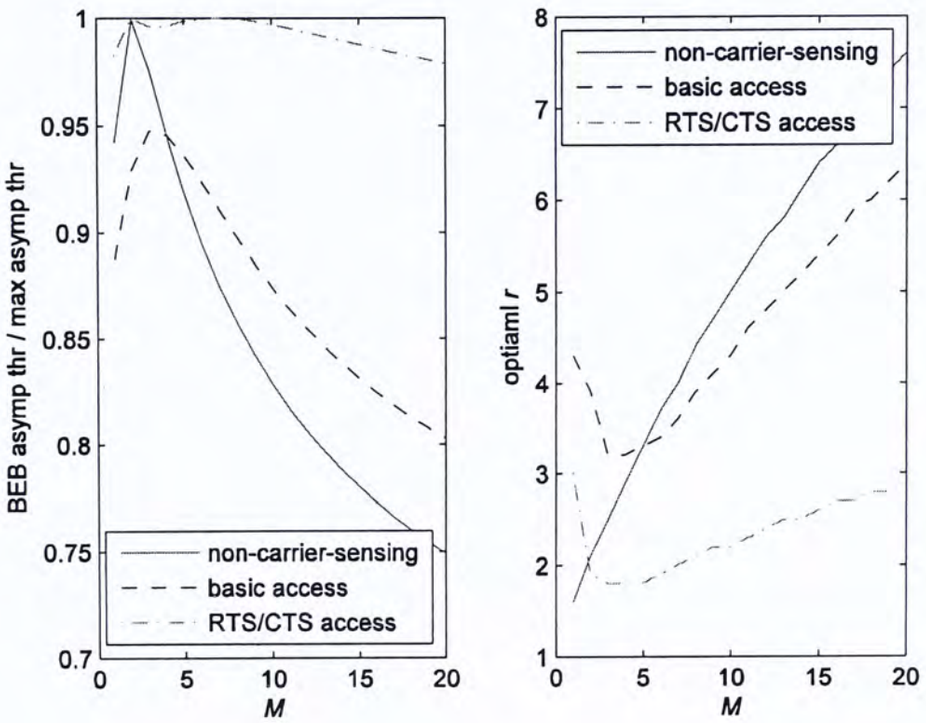

Figure 13 Ratio of BEB asymptotic throughput to maximum asymptotic throughput and optimal r which maximizes the asymptotic throughput versus M for non-carrier-sensing, basic access and RTS/CTS access systems.

By tuning r to the optimal value for each M, we plot the maximum asymptotic throughput against M in Fig. 11. Unlike Fig. 5, in which N is finite, Fig. 11 shows that the maximum asymptotic throughput keeps increasing with M. A close observation of Fig. 11 indicates that the slope of the curve also increases

slowly with M. For example, when $M=1$, the asymptotic throughput is equal to 0.36781. When $M=2$, the asymptotic throughput increases to 0.83991, which is larger than 2 times 0.36781. Such super-linear scalability implies that as M increases, the achievable throughput per unit cost (i.e., bandwidth in CDMA systems or antenna in multi-antenna systems) also increases. This is a strong incentive to consider MPR in future wireless networks.

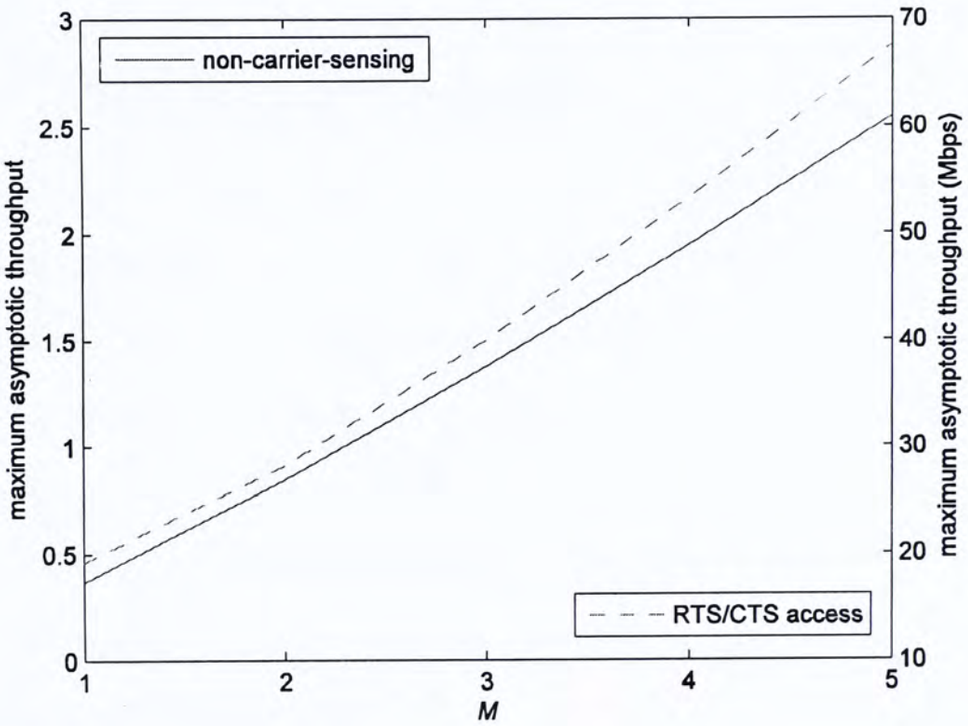

Figure 14 Maximum asymptotic throughput by tuning r versus M for both non-carrier-sensing (corresponding to the left axis) and RTS/CTS access (corresponding to the right axis) systems.

Chapter 6
Carrier-sensing System

6.1 Throughput Derivation

Having studied the performance of EB for non-carrier-sensing systems, whose backoff slot length is simply a constant, we turn to carrier-sensing systems in this chapter. Recall that backoff slot is defined as the variable time interval between two consecutive backoff timer decrements. Its length may be T_i, T_s or T_c for carrier-sensing systems.

For carrier-sensing systems, we again define the throughput S as the ratio of the average payload information bits being transmitted in a backoff slot to the average length of a backoff slot:

$$S = \frac{E[\text{payload information bits transmitted in a backoff slot}]}{E[\text{length of a backoff slot}]}$$

$$= \frac{\sum_{k=1}^{M} kP_{tk}P_{tr}L}{(1-P_{tr})T_i + P_{tr}P_sT_s + P_{tr}(1-P_s)T_c} \qquad (25)$$

where T_s is the backoff slot time spent when there are successful transmissions, T_c is the backoff slot time when there are collisions, $P_s = \sum_{k=1}^{M} P_{tk}$ is the

conditional probability of successful transmissions in a busy time slot, and P_{tr}, P_{tk} and L are already defined in the previous chapter,

6.2 Asymptotic Behavior

To have a clearer picture of the asymptotic behavior of EB for carrier-sensing systems, we again resort to the infinite population model proposed in the last chapter. The straightforward expression for the asymptotic throughput for carrier-sensing systems is

$$\lim_{N\to\infty} S = \frac{\sum_{k=1}^{M} kP_{tk}P_{tr}L}{(1-P_{tr})T_i + P_{tr}P_sT_s + P_{tr}(1-P_s)T_c} \tag{26}$$

where all the symbols have already been defined previously in (25) except that P_{tr} and P_{tk} should be changed to

$$P_{tr} = 1 - P\{X = 0\} = 1 - e^{-\lambda} \tag{27}$$

and

$$P_{tk} = P\{X = k\}/P_{tr} = \frac{\lambda^k}{k!}e^{-\lambda} \Big/ P_{tr} \tag{28}$$

respectively.

As a special case of carrier-sensing systems when $T_c = T_s = T_b$, the throughput S can be simplified as

$$S = \frac{\sum_{k=1}^{M} kP_{tk}P_{tr}L}{(1-P_{tr})T_i + P_{tr}T_b}. \tag{29}$$

Similarly, the asymptotic throughput can also be simplified as

$$\lim_{N\to\infty} S = \frac{\sum_{k=1}^{M} kP_{tk}P_{tr}L}{(1-P_{tr})T_i + P_{tr}T_b}. \tag{30}$$

As a matter of fact, the non-carrier-sensing systems discussed earlier can also be mathematically interpreted as a special case of carrier-sensing systems when all the three time parameters are equal, i.e. $T_i = T_c = T_s = T_{slot}$.

As mentioned earlier in Chapter 2, the IEEE 802.11 DCF can be classified into the category of carrier-sensing systems. For example, the various lengths of a backoff slot for 802.11 DCF basic access scheme are given as

$$\begin{cases} T_i = \sigma \\ T_s = H + L/R + SIFS + \delta + ACK + DIFS + \delta \\ T_c = H + L/R + DIFS + \delta \end{cases} \tag{31}$$

and those for 802.11 DCF request-to-send/clear-to-send (RTS/CTS) access scheme are given as

$$\begin{cases} T_i = \sigma \\ T_s = RTS + SIFS + \delta + CTS + SIFS + \delta + H \\ \qquad + L/R + SIFS + \delta + ACK + DIFS + \delta \\ T_c = RTS + DIFS + \delta \end{cases} \tag{32}$$

where δ is the propagation delay, $H = PHY_{hdr} + MAC_{hdr}$ is the total overhead time to transmit the packet headers, and R is the data rate for payload transmission.

Similar to the discussion in the non-carrier-sensing case, there still exists an optimal r that maximizes the asymptotic throughput with certain MPR capability. To show the influence of system parameters, such as T_i, T_s and T_c, on the asymptotic behavior of EB, we take IEEE 802.11 DCF RTS/CTS access

and basic access as examples. The results shown here are from analytical analysis and the parameter settings we used are basically those from IEEE 802.11g as listed in Table 1, except that there is no retry limit here.

	802.11g
Packet payload	8184 bits
MAC header	272 bits
PHY overhead	26 μs
ACK	112 bits + PHY
RTS	160 bits + PHY
CTS	112 bits + PHY
Basic rate	6 Mbps
Data rate	54 Mbps
Slot time σ	9 μs
SIFS	10 μs
DIFS	28 μs
Propagation delay δ	1 μs

Table 1 System parameters and additional parameters used in numerical analysis.

As shown in Fig. 10, for RTS/CTS access scheme, the asymptotic performance of BEB is very close to optimum for a large variety of M. On the other hand, for basic access, BEB is far from optimum as observed in Fig. 10. Different from non-carrier-sensing systems, the optimal r in carrier-sensing systems is not always increasing as can be seen from this figure. The approach to achieve the best throughput performance by adjusting r in this case is analogous to the one we mentioned in Chapter 4. However, from an engineering point of view, we argue that BEB (i.e., $r = 2$) already achieves a close-to-optimal throughput for RTS/CTS access scheme, while on the other hand tuning r to the optimal is important for basic access scheme. Recall that the MPR MAC protocol introduced in Chapter 3 is based on RTS/CTS access scheme. Since BEB

already achieves close-to-optimum performance in this case, it is employed as the collision resolution scheme in our proposed MPR protocol. Figure 11 shows that about 47% increase in the maximum asymptotic throughput can be achieved when $M = 2$, compared with conventional IEEE 802.11g. Similar to the conclusions we made for non-carrier-sensing systems, it is observed in Fig. 11 that the maximum asymptotic throughput increases super-linearly with M for RTS/CTS access scheme.

Chapter 7

General MPR Model

Our previous analysis has assumed that all simultaneously transmitted packets are successfully received, as long as the number does not exceed M. This model captures the essence of MPR and enables the study of the most fundamental behaviour of EB with MPR. In this chapter, we extend our analysis to a more general reception model, which characterizes realistic phenomena in practical wireless networks, such as capture effects and channel errors. To begin, we define

$$\varepsilon_{n,k} = \Pr\{k \text{ packets are correctly received} | n \text{ are transmitted}\}$$

for $1 \le n \le N,\ 0 \le k \le n$, where N is the total number of users in the network. Then, the so called reception matrix of the channel is given by

$$E = \begin{bmatrix} \varepsilon_{1,0} & \varepsilon_{1,1} & & & & \\ \varepsilon_{2,0} & \varepsilon_{2,1} & \varepsilon_{2,2} & & & \\ \vdots & \vdots & \ddots & \ddots & & \\ \varepsilon_{n,0} & \varepsilon_{n,1} & \cdots & \varepsilon_{n,n-1} & \varepsilon_{n,n} & \\ \vdots & \vdots & \vdots & \vdots & \ddots & \ddots \\ \varepsilon_{N,0} & \varepsilon_{N,1} & \cdots & \cdots & \cdots & \varepsilon_{N,N} \end{bmatrix}. \tag{43}$$

The general MPR collision model is characterized by the reception matrix above, which probabilistically describes successful packet receptions. This model is very general and can be used to model many practical systems. For

example, the reception matrix for the conventional collision model, which allows at most one packet to be successfully received at one time, is given by

$$\varepsilon_{n,k} = \begin{cases} 1 & \text{for } n = 1, k = 1 \text{ or } 2 \le n \le N, k = 0 \\ 0 & \text{otherwise} \end{cases}. \tag{44}$$

As just mentioned, the MPR collision model we consider in all previous chapters is only a special case of the general model. The elements of its reception matrix are given as follows

$$\varepsilon_{n,k} = \begin{cases} 1 & \text{for } 1 \le n \le M, k = n \text{ or } M+1 \le n \le N, k = 0 \\ 0 & \text{otherwise} \end{cases}. \tag{45}$$

Although we have adopted the special MPR collision model of (45) in the preceding chapters of this thesis, our methodology in analyzing the performance of EB can be applied to the general MPR collision model given in (43). To avoid unnecessary repetition, we just list the results for the general case here.

For the general MPR collision model defined in (43), the conditional collision probability p_c is given by

$$p_c = \sum_{k=1}^{N} \binom{N-1}{k-1} p_t^{k-1} (1-p_t)^{N-k} \sum_{i=0}^{k} \varepsilon_{k,i} \left(1 - \frac{i}{k}\right). \tag{46}$$

For non-carrier-sensing systems, the throughput, which is defined as the average payload information bits divided by the length of a backoff slot, is given by

$$S = \frac{\sum_{n=1}^{N} P\{n \text{ packets transmitted}\} \sum_{k=1}^{n} k\varepsilon_{n,k} L}{T_{slot}} = \frac{\sum_{n=1}^{N} \binom{N}{n} p_t^n (1-p_t)^{N-n} \sum_{k=1}^{n} k\varepsilon_{n,k} L}{T_{slot}} . \quad (47)$$

Similarly, for carrier-sensing systems, the throughput is given by

$$S = \frac{\sum_{k=1}^{N} P_{tk} P_{tr} \sum_{i=1}^{k} i\varepsilon_{k,i} L}{(1-P_{tr})T_i + \sum_{k=1}^{N} P_{tk} P_{tr} (1-\varepsilon_{k,0})T_s + \sum_{k=1}^{N} P_{tk} P_{tr} \varepsilon_{k,0} T_c} . \quad (48)$$

Note that the collision probability p_c and the throughput S derived in this chapter depend on the specific reception matrix employed in the general MPR model.

Chapter 8

Conclusions

This thesis has investigated the performance of EB in random-access networks with MPR capability that allows M packets to be simultaneously transmitted without collisions. Extensive simulations have validated the accuracy of our theoretical analysis. Not only does our analysis lay down a theoretical foundation for the performance evaluation of EB with MPR, it is also a useful aid for system design in terms of setting the correct operating parameters.

To be sufficiently general, both carrier-sensing and non-carrier-sensing systems have been studied. In particular, we have derived the throughput expressions for both systems under saturated-traffic condition, and have analyzed the asymptotic behavior of EB with MPR under infinite-population assumption. In both carrier-sensing and non-carrier-sensing systems, the collision probability p_c converges to $1/r$, with r being the exponential backoff factor, regardless of M. With the help of our throughput expression, we have analyzed the effects of M and r on system throughput. Based on the analysis, we argue that the commonly deployed BEB scheme is far from optimum in most systems except the carrier-sensing systems with RTS/CTS four-way handshake. In particular, the optimum r increases with M for large M. We

further note that the asymptotic throughput degrades sharply when r is smaller than the optimum value, while the curve is much flatter when r exceeds the optimum. Therefore, for system robustness, it is preferable to set r large enough to avoid dramatic throughput degradation.

To further illustrate the advantage of MPR, extensive numerical study has been conducted. Our results show that for carrier-sensing systems, throughput improvement of 47% can be achieved with our proposed MPR MAC protocol when $M = 2$, compared with the conventional IEEE 802.11g protocol. For both carrier-sensing and non-carrier-sensing systems, network throughput increases super-linearly with M for the infinite-user-population case. Such scalability provides strong incentives for further investigations on engineering and implementation details of MPR systems.

Having understood the fundamental behavior of MPR, we propose a practical protocol to exploit the advantage of MPR in IEEE 802.11-like WLANs. By incorporating advanced PHY-layer blind detection and MUD techniques, the protocol can implement MPR in a fully distributed manner with marginal modification of MAC layer.

Bibliography

[1] J. Goodman, A. G. Greenberg, N. Madras, and P. March, "Stability of binary exponential backoff," *J. ACM*, vol. 35, no. 3, pp. 579-602, Jul. 1988.

[2] L. Tong, Q. Zhao, and G. Mergen, "Multipacket reception in random access wireless networks: From signal processing to optimal medium access control," *IEEE Commun. Mag.*, vol. 39, no. 11, pp. 108-112, Nov. 2001.

[3] P. B. Rapajic and D. K. Borah, "Adaptive MMSE maximum likelihood CDMA multiuser detection," *IEEE J. Select. Areas Commun.*, vol. 17, no. 12, pp. 2110-2122, Dec. 1999.

[4] S. Talwar, M. Viberg, and A. Paulraj, "Blind separation of synchronous co-channel digital signals using an antenna array, Part I: Algorithms," *IEEE Trans. Signal Processing*, vol. 44, no. 5, pp. 1184-1197, May 1996.

[5] P. X. Zheng, Y. J. Zhang and S. C. Liew, "Multipacket reception in wireless local area networks," *Proc. IEEE ICC'06*, Istanbul, Turkey, June, 2006.

[6] S. Ghez, S. Verdú, and S. Schwartz, "Stability properties of slotted Aloha with multipacket reception capability," *IEEE Trans. Automat. Contr.*, vol. 33, no. 7, pp. 640–649, Jul. 1988.

[7] Q. Zhao and L. Tong, "A multiqueue service room MAC protocol for wireless networks with multipacket reception," *IEEE/ACM Trans. Networking*, vol. 11, pp. 125-137, Feb. 2003.

[8] Q. Zhao and L. Tong, "A dynamic queue protocol for multi-access wireless networks with multipacket reception," *IEEE Trans. Wireless Comm.*, vol. 3, no. 6, pp. 2221-2231, Nov. 2004.

[9] ANSI/IEEE Std 802.3-1985, IEEE standards for local area networks: carrier sense multiple access with collision detection (CSMA/CD) access method and physical layer specifications, 1985.

[10] IEEE Std 802.11-1997, IEEE Std 802.11-1997 Information Technology-telecommunications And Information exchange Between Systems-Local And Metropolitan Area Networks-specific Requirements-part 11: Wireless Lan Medium Access Control (MAC) And Physical Layer (PHY) Specifications, Nov. 1997.

[11] B. J. Kwak; N. O. Song, and L. E. Miller, "Performance analysis of exponential backoff," *IEEE/ACM Trans. Networking*, vol. 13, no. 2, pp. 343-355, Apr. 2005.

[12] G. Bianchi, "Performance analysis of the IEEE 802.11 distributed coordination function," *IEEE J. Select. Areas Commun.*, vol. 18, no. 3, pp. 535-547, Mar. 2000.

[13] C.B. Papadias, A.J. Paulraj, "A constant modulus algorithm for multiuser signal separation in presence of delay spread using antenna arrays," *IEEE Signal Processing Letters*, vol. 4, no. 6, pp. 178-181, June 1997.

[14] S. Talwar, M. Viberg, and A. Paulraj, "Blind estimation of multiple co-channel digital signals using an antenna array," *IEEE Signal Processing Letters.*, vol. 2, no. 1, pp. 29-31, Feb. 1994.

[15] P. X. Zheng, Y. J. Zhang and S. C. Liew, "Analysis of Exponential Backoff with Multipacket Reception in Wireless Networks," *Proc. of the IEEE Conference on Local Computer Networks (LCN) 2006*, Tampa, U.S.A., Nov. 2006.

[16] N. Abramson, "The ALOHA system-Another alternative for computer communications," in *1970 Fall Joint Comput. Conf., AFIPS Conf. Proc.*, vol. 37. Alontvale, N. J.: AFIPS Press, 1970, pp. 281-285.

[17] L. Kleinrock and S. S. Lam, "Packet switching in a multiaccess broadcasting channel: Performance evaluation," *IEEE Trans. Commun.*, vol. COM-23, pp. 410-423, Apr. 1975.

[18] A. B. Carleial and M. E. Hellman, "Bistable behavior of ALOHA-type systems," *IEEE Trans. Commun.*, vol. COM-23, pp. 401-410, Apr. 1975.

[19] H. Kobayashi, Y. Onozato, and D. Huynh, "An approximate method for design and analysis of an ALOHA system," *IEEE Trans. Commun.*, vol. COM-25, pp. 148-158, Jan. 1977.

[20] Y.-C. JENQ, "On the Stability of Slotted ALOHA Systems," *IEEE Trans. Commun.*, vol. COM-28, no. 11, pp. 1936-1939, Nov. 1980.

[21] G. Bianchi, L. Fratta, and M. Oliveri, "Performance analysys of IEEE 802.11 CSMA/CA medium access control protocol," in Proc. IEEE PIMRC, pp. 407–411, Taipei, Taiwan, Oct. 1996.

[22] B. P. Crow, I. Widjaja, L. G. Kim, and P. T. Sakai, "IEEE 802.11 Wireless Local Area Networks," *IEEE Commun. Mag.*, vol. 35, no. 9, pp. 116-126, Sept. 1997.

[23] F. Cali, M. Conti, and E. Gregori, "IEEE 802.11 wireless LAN: Capacity analysis and protocol enhancement," *INFOCOM'98*, San Francisco, CA, Mar. 1998.

[24] G. Bianchi, "IEEE 802.11—Saturation throughput analysis," *IEEE Commun. Lett.*, vol. 2, pp. 318–320, Dec. 1998.

[25] Y. Xiao and J. Rosdahl, "Throughput and Delay Limits of IEEE 802.11," *IEEE Commun. Lett.*, vol. 6, no. 8, pp. 355–57, Aug. 2002.

[26] Y. Xiao and J. Rosdahl, "Performance Analysis and Enhancement for the Current and Future IEEE 802.11 MAC Protocols," *ACM Sigmobile Mobile Comp. and Commun. Rev.*, vol. 7, no. 2, pp. 6–19, Apr. 2003.

[27] D. J. Aldous, "Ultimate instability of exponential back-off protocol for acknowledgment-based transmission control of random access communication channels," *IEEE Trans. Inform. Theory*, vol. 33, no. 2, pp. 219–223, Mar. 1987.

[28] D. G. Jeong and W. S. Jeon, "Performance of an exponential backoff scheme for slotted-ALOHA protocol in local wireless environment," *IEEE Trans. Veh. Technol.*, vol. 44, no. 3, pp. 470–479, Aug. 1995.

[29] K. Sakakibara, T. Seto, D. Yoshimura, and J. Yamakita, "On the stability of slotted ALOHA systems with exponential backoff and retransmission cutoff in slow-frequency-hopping channels," in *Proc. 4th Int. Symp. Wireless Personal Multimedia Communications*, Aalborg, Denmark, Sep. 2001.

[30] H. Al-Ammal, L. A. Goldberg, and P. MacKenzie, "An improved stability bound for binary exponential backoff," *Theory Comput. Syst.*, vol. 30, pp. 229–244, 2001.